EPJ manuscript No.
(will be inserted by the editor)

Foam improved oil recovery: Modelling the effect of an increase in injection pressure

Elizabeth Mas Hernández[1], Paul Grassia[2,3], and Nima Shokri[1]
[1] CEAS, The Mill, University of Manchester, Oxford Rd, Manchester M13 9PL, UK
[2] Chemical & Process Engng, University of Strathclyde, James Weir Bldg, 75 Montrose St, Glasgow G1 1XJ, UK
[3] Ciencias Matemáticas y Físicas, Universidad Católica de Temuco, Rudecindo Ortega 02950, Temuco, Chile

Received: date / Revised version: date

Abstract. A model, called pressure-driven growth, is analysed for propagation of a foam front through an oil reservoir during improved oil recovery using foam. Numerical simulations of the model predict, not only the distance over which the foam front propagates, but also the instantaneous front shape. A particular case is studied here in which the pressure used to drive the foam along is suddenly increased at a certain point in time. This transiently produces a concave front shape (seen from the domain ahead of the front): such concavities are known to be delicate to handle numerically. As time proceeds however, the front evolves back towards a convex shape, and this can be predicted by a long-time asymptotic analysis of the model. The increase in driving pressure is shown to be beneficial to the improved oil recovery process, because it gives a more uniform sweep of the oil reservoir by foam.

PACS. 82.70.Rr Foams – 47.56.+r Porous materials, flow through – 89.30.aj Petroleum

1 Background

When extracting oil from an underground reservoir, the amount of oil recovered can be increased by injecting a displacing fluid into the reservoir under pressure. Foam is known to have advantages over other choices of displacing fluid (e.g. gas injection or water injection) since foam tends to give a more even sweep/displacement [1–3].

Rather than direct injection of foam into an oil reservoir, improved oil recovery often uses so called surfactant alternating gas. In that process, foam is produced in situ in the reservoir by injection of surfactant solution followed by gas [2,4]. There is a wet foam front containing small bubbles formed where the gas meets the surfactant. Typically the thickness of this wet foam front is much less than the distance over which it propagates. Moreover most of the dissipative resistance to the foam motion is known to be located in this wet foam region [2].

Shan and Rossen [2] proposed a simple idealised model for the foam motion where *all* the resistance is assumed to be contained in the wet foam region. This model has been termed 'pressure-driven growth' [5] and it allows the prediction of how the shape of the wet foam front evolves over time [6]. The model (in its simplest form) assumes that an element of foam front moves in a direction that is normal to the front and at a speed that is proportional to the difference between the driving injection pressure and the background hydrostatic pressure in the reservoir, the latter increasing with depth.

This implies that the speed of the front decreases with increasing depth. The dissipative wet foam zone is also known [2,5,7] to spread out proportionally to the distance the front travels (albeit with a coefficient of proportionality much smaller than unity). This leads to further reductions in the speed of the foam front over time.

The model is most compactly described in dimensionless position and time variables (denoted in what follows via a subscript 'D'). Specifically length scales are made dimensionless [2,5] by dividing through by $P_{drive}/(\Delta\rho\, g)$ where P_{drive} is the pressure initially used to drive the foam along, $\Delta\rho$ is the density difference between the injected surfactant solution and the injected gas, and g is the acceleration due to gravity. Meanwhile time scales are made dimensionless [2,5] by dividing through by the quantity $(1-S_w)\,\phi\, P_{drive}\,\tau/(k\,\lambda_r\,\Delta\rho^2\,g^2)$ where S_w is the liquid fraction in the foam (generally considerably smaller than unity), ϕ is the reservoir porosity, τ is the ratio between the thickness of the wet foam front and the distance over which it propagates (τ is expected to be nearly constant [2]), k is the reservoir permeability, and λ_r is the relative mobility of the wet foam front. In the 'typical' example presented by Shan and Rossen [2], 1 unit of dimensionless distance corresponds to around 300 m and 1 unit of dimensionless time corresponds to 14 days. In dimensionless form, the governing system of differential equations (1)–(5) for this process known as pressure-driven growth describes the evolution of the foam front inside a homogeneous and isotropic reservoir (the simplest case) during

improved oil recovery [2,5]:

$$\frac{\mathrm{d}X_D}{\mathrm{d}t_D} = \frac{(1-Z_D)\cos\alpha}{s_D} \tag{1}$$

$$\frac{\mathrm{d}Z_D}{\mathrm{d}t_D} = \frac{(1-Z_D)\sin\alpha}{s_D} \tag{2}$$

$$\mathrm{d}s_D/\mathrm{d}t_D = \sqrt{(\mathrm{d}X_D/\mathrm{d}t_D)^2 + (\mathrm{d}Z_D/\mathrm{d}t_D)^2} \tag{3}$$

$$X_D(Z_D,0) = s_D(Z_D,0) = s_{D_0} \tag{4}$$

$$\alpha(0,t_D) = 0 \tag{5}$$

which are actually equivalent to Eqs. (2.10)–(2.11), (2.13) and (2.18) of [5]. Here X_D is the horizontal position in a rectangular reservoir, Z_D the vertical position downwards, t_D is the time, s_D the distance that a material point on the front travels, s_{D_0} is a value much smaller than unity that we chose as $s_{D_0} = 0.001$ (which can be taken to represent the initial thickness of the wet foam front relative to its initial length), and α the angle giving the orientation of the front normal with respect to the horizontal (which can be determined given the position of a material point on the front and its neighbours). Note that whereas equations (1)–(3) apply to front material points, specifying Z_D at any given t_D is sufficient to fix a material point, so that X_D and s_D can alternatively be written as functions of the two arguments Z_D and t_D, and this is reflected in the notation used in equations (4)–(5).

Equations (1)–(2) are specific to the case of a unit driving pressure (in dimensionless units) corresponding to a front that penetrates to a unit depth below the surface: in dimensional units this corresponds to the depth that matches the injection pressure to the hydrostatic pressure in the system. Note that, by design, the driving pressure is chosen such that the penetration depth for the foam front is at least as large as the depth at which the oil is located. There can however [6] be gains in choosing a penetration depth substantially larger than that (corresponding then to the oil being located in just a small fraction of one dimensionless depth unit). One advantage of this is that (upon converting back to dimensional variables) the distance over which the front propagates is greater at any given time. Another advantage of choosing a larger penetration depth is that it reduces the amount of so called 'gravity override' [2]. If the front is highly inclined across the region where the oil is located, then the leading edge of the front has run far ahead other parts of the front that are still sweeping oil: in effect some oil is being left behind. However if driving pressure is higher and the front is close to vertical across the region where the oil is located, the sweep is more uniform and hence considered to be more efficient.

Numerical and analytical solutions for equations (1)–(5) give a front described by convex curves in a two-dimensional X_D vs Z_D plot. This is fortunate because the equations governing pressure-driven growth are well behaved in the case of convex shapes, whereas to handle concave shapes [5], special strategies need to be put in place for solving the equations. Unfortunately there are a number of scenarios (generalisations of the simple homogeneous, isotropic, unit driving pressure case that is discussed above) for which the foam front will no longer be convex, instead concavities will appear [5,8]. Amongst these is the case of a sudden rise in the driving pressure which is what is considered here.

The remainder of this study is laid out as follows. Section 2 introduces the case where the driving pressure is variable, presenting the equations that are used, along with explanation about how those equations are implemented in a computer program. Section 3 gives more detail on the parameter values used in the numerical solution and the results obtained for the foam front displacement. Section 4 presents an analytical solution for the foam front shape at long time, and quantifies how this shape changes in response to changing pressure. Finally, Section 5 offers conclusions.

2 Increase in pressure

The whole idea of improved oil recovery processes is maintaining the pressure necessary for production in the reservoir. Unfortunately the production rate is not constant over the course of the process. In particular (as was mentioned earlier) the dissipative wet foam front spreads out over time [2,5,7], albeit still maintaining a thickness that is smaller than the distance over which the front propagates. If the driving pressure is held fixed as the dissipative wet foam front thickens, the front propagation speed must fall. A production engineer could respond to this falling rate by raising the driving pressure[1]. Thus, after some time during the displacement of a foam front, a higher pressure than the one used at the start of the operation might be required. The higher pressure may also have the additional benefit of reducing the amount of gravity override, bringing the foam front closer to vertical across the region where the oil is located.

Here we consider how this increase in the driving pressure will affect the shape of the foam front that has been described above. As has been postulated in [5], we expect that the pressure increase will introduce concavities on the curves as shown schematically in Fig. 1. Such concavities are known to be problematic for implementation of the pressure-driven growth model and special techniques are required to handle them [5]. Basically the concavity (once it becomes sufficiently sharp) needs to be propagated at a higher velocity than surrounding parts of the front to avoid the appearance of spurious loops in the front shape.

The equations describing horizontal and vertical front velocity must moreover include a term for the relative pressure increase P_i, that is imposed after some time that we specify as t_p. The modified equations are shown below

$$\frac{\mathrm{d}X_D}{\mathrm{d}t_D} = \frac{(1+P_i-Z_D)\cos\alpha}{s_D} \tag{6}$$

[1] Shan and Rossen [2] in fact studied some cases where pressure was continually increased over time to hold injection rate fixed – see Figs. 24(a) and 25(a) in the cited reference.

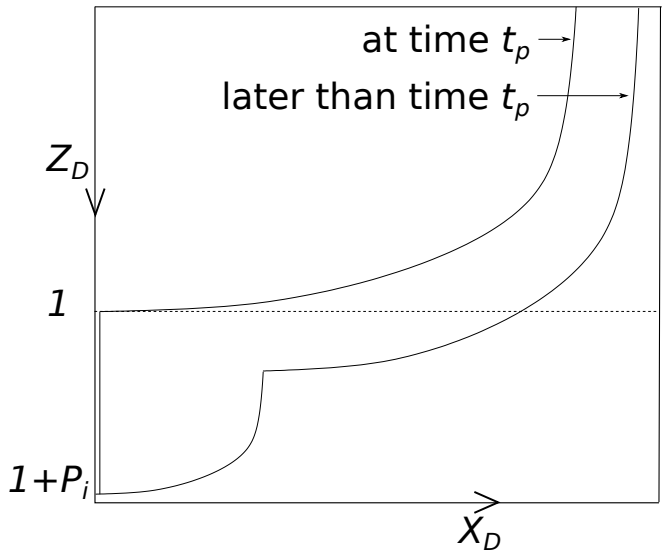

Fig. 1. Schematic of foam front shape in coordinates X_D vs Z_D with an increase in driving pressure. For a front material point, both X_D and Z_D are functions of time t_D. At a certain time t_p pressure is raised so as to become $1 + P_i$ times the original pressure.

$$\frac{\mathrm{d}Z_D}{\mathrm{d}t_D} = \frac{(1 + P_i - Z_D)\sin\alpha}{s_D} \tag{7}$$

where the other variables have been described previously in Section 1.

The X_D and s_D values at the top of the front are given by Eq. (8), which is obtained with the aid of the boundary condition, Eq. (5),

$$\begin{aligned} X_D(0, t_D) &= s_D(0, t_D) \\ &= \sqrt{2(1 + P_i)(t_D - t_p) + 2t_p + s_{D_0}^2}. \end{aligned} \tag{8}$$

As depicted in Fig. 1, the pressure increase will also affect the depth to which the foam front extends, for this reason it is necessary to give initial conditions for this region, $1 < Z_D < 1 + P_i$ (recall that the maximum vertical dimensionless distance has been unity up till now). Hence, initial conditions for this vertical interval will satisfy $X_D = s_D = s_{D_0}$ at $t_D = t_p$; and from there we will follow the advance of the front.

This case has been implemented numerically with Matlab via a discretised representation of the foam front. Here we describe the changes that have been done to the computer code used originally for a constant driving pressure (the algorithm for the constant pressure case having been described already in literature [5]). First of all, it is necessary to specify the values of the new parameters t_p and P_i. Then, new variables (i.e. points on the foam front) used in calculations are set for vertical positions $1 < Z_D < 1 + P_i$ at time t_p. Discrete positions of points (X_D, Z_D) are used to obtain segment orientations (angle α), and then it is possible to calculate velocities for each point.

Calculation of the speed of the front advance is performed using a conditional construction in the following way: if $t_D < t_p$, Eqs. (1)–(2) are used; on the other hand, if $t_D \geq t_p$, the code checks for the sign of front curvature (K) and magnitude of turning angle (θ) between adjacent segments[2] and applies either Eqs. (6)–(7) for $K > 0$ and/or θ less than a specific value (specified here as θ_{sharp}), or (9)–(10) for $K < 0$ and $\theta > \theta_{sharp}$

$$\frac{\mathrm{d}X_D}{\mathrm{d}t_D} = \frac{(1 + P_i - Z_D)\cos\alpha}{s_D \cos\frac{\theta}{2}} \tag{9}$$

$$\frac{\mathrm{d}Z_D}{\mathrm{d}t_D} = \frac{(1 + P_i - Z_D)\sin\alpha}{s_D \cos\frac{\theta}{2}} \tag{10}$$

where the additional term in the denominator, compared to (6)–(7), speeds up the displacement of concave regions correcting the velocity of points there. The reasons for needing to do this are explained at length in [5]: physically the reason is that front material points travel at different speed from 'shocks', i.e. corners or cusps (into which concave regions develop). Such 'shocks' arise because the pressure-driven growth is a singular limit of a more general model called the 'viscous froth'[3] which is well known in the foam physics literature [9,10]. Note that the corner shown on Fig. 1, which joins points originally in $Z_D < 1$ to points newly set in motion in $Z_D > 1$ will always be propagated via Eqs. (9)–(10) (at least for any reasonable choice of the value of θ_{sharp}). Careful consideration has been given in the literature regarding how to choose values of θ_{sharp}, with any value chosen significantly smaller than unity being deemed suitable for keeping otherwise problematic concavities localised and contained [5].

The values of X_D and s_D at the top are calculated with a conditional construction also, where Eq. (8) is used if $t_D \geq t_p$, but $X_D(0, t_D) = \sqrt{2t_D + s_{D_0}^2}$ applies if $t_D < t_p$.

The next section presents results obtained from these modifications to the program.

3 Results

For the numerical solution of the displacement of foam for increase in the driving pressure at a certain $t_D = t_p$, a Heun method is used. The front is discretised by setting 200 intervals along the Z_D axis, the time step used is chosen as 1×10^{-5}, front segments at the top are split when they grow up to a length of 0.05 (to avoid having excessively long intervals and keep a fair representation of the curves at the top), short segments are removed when they decrease to a length of 0.002 (helping to avoid formation of spurious loops [5]), $\theta_{sharp} = \pi/18$, $t_p = 1$ and $P_i = 0.2$: these values have been chosen arbitrarily for the purpose of illustrating the model.

[2] Determining curvature and angle between segments is necessary for handling concavities: see [5] for more details on this matter.

[3] Realising the analogy between pressure-driven growth and viscous froth is non-trivial [5], as one model describes the advance of an entire foam front on a reservoir engineering scale and the other describes individual foam films on a much smaller scale.

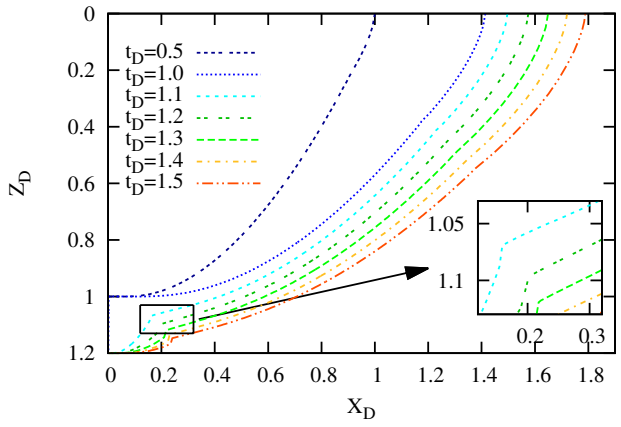

Fig. 2. Foam front for pressure increase with $t_p = 1$ and $P_i = 0.2$, for $0.5 \leq t_D \leq 1.5$. The inset shows a zoomed view.

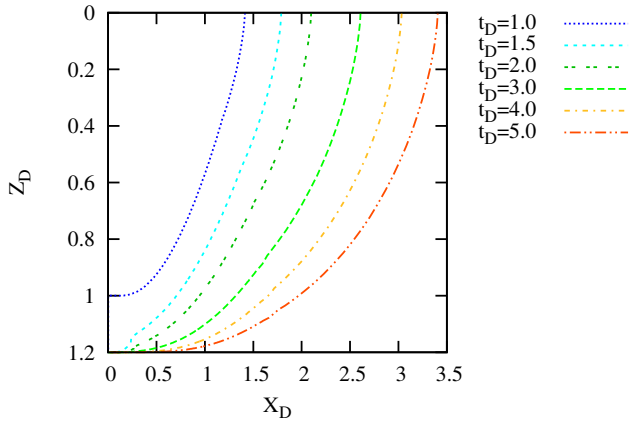

Fig. 3. Foam front for pressure increase with $t_p = 1$, $P_i = 0.2$, for $1 \leq t_D \leq 5$.

The foam front obtained with the above mentioned values is presented in Fig. 2: it is observed that the pressure increase leads to formation of concavities. There is a clear concave corner or cusp, separating points that have been moving continuously since the start of the process from those that have only newly been set in motion at time t_p. These results also confirm a suggestion by Grassia et al. [5] that points in the proximity of the cusp (formed due to a sudden increase in pressure) could have negative curvature[4]. In fact, some points above and to the right of the cusp have negative curvature for the curves in Fig. 2: although this is difficult to see even on the zoomed inset in that plot. The reason why those negative curvature points appear is because points immediately to the right of the cusp have historically displaced less distance than points further to the right. Since the thickness of (and hence the dissipation of) the wet foam front grows according to the displacement, points immediately to the right of the cusp

[4] The fact that some points have a negative curvature just to the right of the cusp also corroborates a finding by Shan and Rossen [2], in their Figs. 24(a) and 25(a).

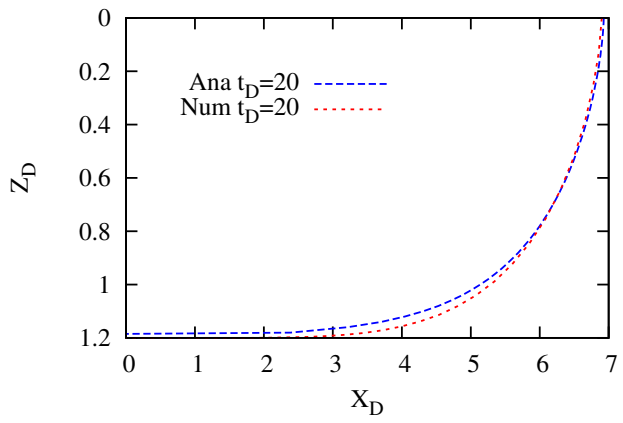

Fig. 4. Foam front for analytical and numerical results with $P_i = 0.2$. For the numerical computations $t_p = 1$.

move faster than those further to the right (owing to the $1/s_D$ factor in Eqs. (6)–(7)): this then produces negative curvature (transiently). Subsequently, these negative regions eventually focus down into the cusp itself.

Figure 3 presents data for a longer t_D interval, where it is shown that after a while the concavity becomes less significant and indeed (after $t_D \approx 3$ in this case) the concavity is pushed virtually to the bottom of the front where the front is barely advancing any more, and so the shape is dominated by the convex part of the front higher up, which corroborates the findings presented in [8].

As we have seen, over time concavities tend to be pushed right to the bottom of the solution domain, and the foam front is dominated by a convex front shape higher up. It is possible to obtain an analytical solution for the (convex) foam front through an asymptotic analysis, which is presented in the following section.

4 Asymptotic analysis

Here we present the asymptotic analysis of the system of Eqs. (6)–(7) which gives the shape of the foam front for long times.

We define

$$\xi_p = X_D - X_D(0, t_D) \tag{11}$$

where ξ_p is the displacement from the topmost point of the front to an arbitrarily chosen point X_D. The subscript 'p' on ξ_p is to remind us that the solutions depend on driving pressure. By definition ξ_p is negative, since the topmost point displaces the furthest.

At long times, $t_D \gg 1$, the value for $X_D(0, t_D)$ and $s_D(0, t_D)$ given by Eq. (8), can be simplified to

$$X_D(0, t_D) = s_D(0, t_D) \approx \sqrt{2(1 + P_i)t_D} \tag{12}$$

where the terms t_p and s_{D_0} in Eq. (8) are now negligible. Therefore, Eqs. (6)–(7) and (11) can be written

$$\frac{\mathrm{d}X_D}{\mathrm{d}t_D} = \frac{(1 + P_i - Z_D)\cos\alpha}{\sqrt{2(1 + P_i)t_D}} \tag{13}$$

$$\frac{\mathrm{d}Z_D}{\mathrm{d}t_D} = \frac{(1+P_i-Z_D)\sin\alpha}{\sqrt{2(1+P_i)t_D}} \tag{14}$$

$$\xi_p = X_D - \sqrt{2(1+P_i)t_D} \tag{15}$$

where we have introduced an approximation [5] that (for the purposes of computing velocities) at leading order, all points on the foam front displaced through the same distance $s_D(0,t_D)$ as the topmost point.

To simplify the expressions above, we define the following modified variables:

$$\xi_{mod} = \xi_p/(1+P_i), \quad Z_{D_{mod}} = Z_D/(1+P_i), \tag{16}$$

and an expression for $\mathrm{d}Z_{D_{mod}}/\mathrm{d}\xi_{mod}$ can be obtained:

$$\frac{\mathrm{d}Z_{D_{mod}}}{\mathrm{d}\xi_{mod}} = \frac{1-Z_{D_{mod}}}{\sqrt{1-(1-Z_{D_{mod}})^2}} \tag{17}$$

which is an equivalent expression to the one obtained for the case of constant pressure reported by Grassia et al. [5]; the integral of which is,

$$\begin{aligned} -\xi_{mod} = &-\sqrt{1-(1-Z_{D_{mod}})^2} \\ &+\log\left(1/(1-Z_{D_{mod}})\right) \\ &+\log\left(1+\sqrt{1-(1-Z_{D_{mod}})^2}\right) \end{aligned} \tag{18}$$

which in turn, gives

$$\begin{aligned} -\frac{\xi_p}{1+P_i} = &-\sqrt{1-(1-Z_D/(1+P_i))^2} \\ &+\log\left((1+P_i)/(1+P_i-Z_D)\right) \\ &+\log\left(1+\sqrt{1-\left(1-\frac{Z_D}{1+P_i}\right)^2}\right). \end{aligned} \tag{19}$$

Equation (19) is thus a rescaled version of Eq. (4.9) in [5].

Now, given a range of Z_D values, the time t_D and the pressure increase P_i, it is possible to obtain the corresponding X_D using Eqs. (15) and (19). Results for analytical calculations are presented in Fig. 4, where they are compared to numerical results, both for $t_D = 20$. Note that the asymptotic analytical shape is slightly higher up in the reservoir than the numerical one: by construction, the asymptotic shape only attains the lowermost point $Z_D = 1 + P_i$ as $X_D \to -\infty$, i.e. at horizontal locations that are arbitrarily far behind the leading edge at the top of the front.

4.1 Unswept area

In oil recovery applications, once foam begins to exit from a production well, one quantity of interest to the reservoir engineer is the 'unswept area' [5], i.e. the amount of area underneath the foam front (measured from the leading edge at the top) where foam has not yet reached to displace liquid. Areas here are made dimensionless on the scale $P_{drive}^2/(\Delta\rho^2\, g^2)$ where recall P_{drive} is the driving pressure, $\Delta\rho$ is a density difference (between injected surfactant solution and injected gas) and g is acceleration due to gravity. The lower the unswept area, the more efficient the reservoir sweep by foam, i.e. gravity override is reduced.

We consider two distinct cases. In the first case (to be discussed further in Sections 4.2 and 4.3), we suppose that the driving pressure has initially been set at the level such that the maximum penetration depth of the foam front corresponds to the greatest depth at which oil is located: as mentioned previously, the initial driving pressure would not be set any lower than that. We then define the unswept area by $A_u = \int_0^1 |\xi_p|\,\mathrm{d}Z_D$, where (to permit a fair comparison between cases with different values of P_i) the integration proceeds only to the maximum front depth *prior to* imposing a pressure increase. In other words, the integration does not extend all the way to the bottom of the front after pressure increase, as indeed the front now extends even further down than the depth to which the oil is located [6]. In the second case (discussed in more detail in Section 4.4), we suppose that the driving pressure has initially been set such that the maximum penetration depth (even prior to any pressure increase) is a factor D_{max} times larger than the greatest depth at which oil is located, with the parameter $D_{max} \gg 1$. The consequent definition of A_u becomes $A_u = \int_0^{1/D_{max}} |\xi_p|\,\mathrm{d}Z_D$. Now the integration does not extend all the way to the bottom of the front, even before the pressure increase: it only extends down as far as the oil itself extends, i.e. $1/D_{max}$ dimensionless units.

In the first case it is possible to calculate the unswept area for a given pressure increase as[5]

$$A_u = \int_0^1 |\xi_p|\,\mathrm{d}Z_D = (1+P_i)^2 \int_0^{1/(1+P_i)} -\xi_{mod}\,\mathrm{d}Z_{D_{mod}}. \tag{20}$$

Using, for example, $P_i = 0.2$ (as in Figs. 2–3) and integrating numerically Eq. (20) with Simpson's rule (using 10 intervals[6]), the unswept area is $A_u = 0.534$, which is a smaller value than for the constant pressure case, where the unswept area is $\pi/4$ (see [5]); hence the foam front sweep is more efficient with an increase in pressure. Figure 5 plots the unswept area (A_u) against relative increase in pressure (P_i). Unswept area decreases as P_i increases, because a larger pressure increase will make the foam front at any given depth displace further, so the area left unswept will be smaller.

Furthermore, we can obtain asymptotic expressions for A_u in the cases of small and large P_i as explained below.

[5] In the present work we only consider a 2-dimensional foam displacement. In the case of an axisymmetric displacement about a production well, the 'unswept area' would be replaced by an 'unswept volume'. This is readily calculated [5] by multiplying the 'unswept area' by the perimeter of the leading edge of the foam front. This perimeter is given by 2π times Eq. (12).

[6] Using more intervals, e.g. 20 or 30, shows a very close agreement to using 10 intervals.

4.2 The small P_i limit

If $P_i \ll 1$, the right hand side of Eq. (20) becomes:

$$(1+P_i)^2 \left(\int_0^1 -\xi_{mod}\, \mathrm{d}Z_{D_{mod}} - \int_{1/(1+P_i)}^1 -\xi_{mod}\, \mathrm{d}Z_{D_{mod}} \right) \tag{21}$$

where the first integral in the bracket is [5]:

$$\int_0^1 -\xi_{mod}\, \mathrm{d}Z_{D_{mod}} = \frac{\pi}{4}. \tag{22}$$

The integration range of the second integral remains close to one (since P_i is assumed small). When $Z_{D_{mod}}$ is close to one (towards the bottom of the foam front)[5]:

$$-\xi_{mod} \approx -1 + \log\left(2/(1-Z_{D_{mod}})\right) \tag{23}$$

making the second integral in (21) become:

$$\int_{1/(1+P_i)}^1 -\xi_{mod}\, \mathrm{d}Z_{D_{mod}} = \frac{P_i}{1+P_i} \log\left(\frac{2(1+P_i)}{P_i}\right). \tag{24}$$

The unswept area for this small P_i case is then

$$A_u = (1+P_i)^2 \left[\frac{\pi}{4} - \frac{P_i}{1+P_i} \log\left(\frac{2(1+P_i)}{P_i}\right) \right] \tag{25}$$

which in turn can be written as:

$$A_u \approx \frac{\pi}{4} - P_i \log\left(1/P_i\right) + \text{corrections of order } P_i \text{ or smaller.} \tag{26}$$

From (26) it can be observed that the term $P_i \log(1/P_i)$ vanishes as $P_i \to 0$, but its derivative is infinite. This is why Fig. 5 shows a very sharp decrease in A_u as P_i increases near $P_i = 0$.

4.3 The large P_i limit

In the case of a large P_i the integration range in Eq. (20) includes only $Z_{D_{mod}}$ values much smaller than unity. In that domain [5],

$$\xi_{mod} \approx -\frac{2\sqrt{2}}{3} Z_{D_{mod}}^{3/2}. \tag{27}$$

Substituting Eq. (27) into the right hand side of (20), integrating and evaluating the limits, an expression for A_u is obtained for this case:

$$A_u \approx \frac{4\sqrt{2}}{15}(1+P_i)^{-1/2}. \tag{28}$$

Figure 6 compares unswept area obtained from Simpson's rule and analytical results using Eqs. (25), (26) and (28). Here it can be observed that results from Eqs. (25) and (26) match Simpson's rule computations for values of P_i close to $P_i = 0$, whereas predictions from Eq. (28) are close to the Simpson's rule results for larger values of P_i.

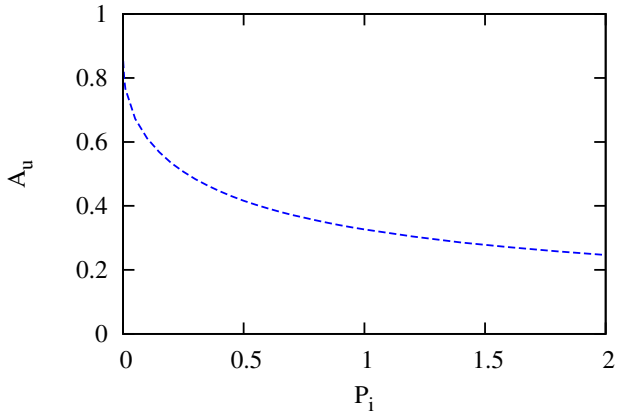

Fig. 5. Unswept area A_u (obtained via Simpson's rule applied to Eq. (20)) versus P_i. Here the initial driving pressure for the foam front is set such that, prior to pressure increase, the front only penetrates to the same depth as the oil.

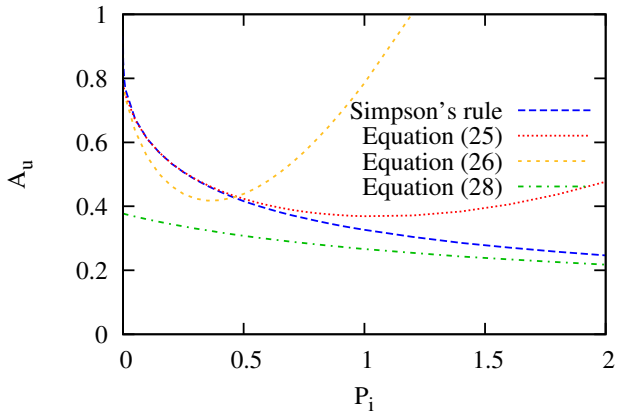

Fig. 6. Comparison between Simpson's rule determination of unswept area and asymptotic analytical formulae. Equations (25) and (26) apply for small P_i values, and Eq. (28) for large P_i values. As in Fig. 5, prior to pressure increase, the front only penetrates to the same depth as the oil.

This completes our discussion of the first case for which the penetration depth of the foam front (prior to any pressure increase) is chosen to match the depth to which the oil is located. The next section treats the second case, for which the initial penetration depth of the foam front is D_{max} times greater than the depth to which oil is located, with $D_{max} \gg 1$. The penetration depth following pressure increase then becomes larger still.

4.4 The large D_{max} limit

As mentioned in Section 4.1, in the case $D_{max} \gg 1$, we evaluate A_u via

$$A_u = \int_0^{1/D_{max}} |\xi_p| \, \mathrm{d}Z_D = (1+P_i)^2 \int_0^{1/(D_{max}(1+P_i))} |\xi_{mod}| \, \mathrm{d}Z_{D_{mod}}. \quad (29)$$

Substituting for ξ_{mod} from equation (27) and integrating we obtain

$$A_u = \frac{4\sqrt{2}}{15}(1+P_i)^{-1/2} D_{max}^{-5/2}. \quad (30)$$

Relative to the situation prior to pressure increase, A_u has decreased by a factor $(1+P_i)^{1/2}$ although it should be remembered that both before and after pressure increase, A_u is actually very small (being of order $D_{max}^{-5/2}$ with $D_{max} \gg 1$).

5 Conclusions

We have presented numerical and analytical results, using the pressure-driven growth model, for a case with a sudden increase in the driving pressure during the process of foam improved oil recovery. The rise in pressure causes the formation of concavities in the curves representing the foam front displacement. To obtain the correct foam front shape and avoid spurious numerical behaviour, these concavities need to be handled specially in our numerical schemes, which were adapted successfully from schemes we have implemented previously [5]. At sufficiently long times the concavities migrate right to the bottom of the solution domain, and a convex front shape is recovered everywhere else. A long-time asymptotic solution has been developed, from which it was possible to calculate the area left unswept by the foam front. The higher the driving pressure, the lower the unswept area, implying a more uniform foam front displacement.

Acknowledgements

EMH acknowledges scholarship funding from the EPS-CONACyT programme. PG acknowledges funding from CONICYT Chile (folio 80140040).

References

1. L. L. Schramm and J. J. Novosad. Micro-visualization of foam interactions with a crude oil. *Colloids and Surf.*, 46:21–43, 1990.
2. D. Shan and W. R. Rossen. Optimal injection strategies for foam IOR. *SPE J.*, 9:132–150, 2004.
3. E. Ashoori, T. L. M. van der Heijden, and W. R. Rossen. Fractional-flow theory of foam displacements with oil. *SPE J.*, 15:260–273, 2010.
4. A. Afsharpoor, G. S. Lee, and S.I. Kam. Mechanistic simulation of continuous gas injection period during surfactant-alternating-gas (SAG) processes using foam catastrophe theory. *Chem. Engng Sci.*, 65:3615–3631, 2010.
5. P. Grassia, E. Mas-Hernández, N. Shokri, S. J. Cox, G. Mishuris, and W. R. Rossen. Analysis of a model for foam improved oil recovery. *J. Fluid Mech.*, 751:346–405, 2014.
6. R. M. de Velde Harsenhorst, A. S. Dharma, A. Andrianov, and W. R. Rossen. Extension and verification of a simple model for vertical sweep in foam surfactant-alternating-gas displacements. *SPE Reservoir Evaluation & Engg*, 17:373–383, 2014.
7. W. R. Rossen, S. C. Zeilinger, J. X. Shi, and M. T. Lim. Simplified mechanistic simulation of foam processes in porous media. *SPE J.*, 4:279–287, 1999.
8. E. Mas-Hernández, P. Grassia, and N. Shokri. Foam improved oil recovery: Foam front displacement in the presence of slumping. *Colloids and Surf. A: Physicochem. and Engg Aspects*, 473:123–132, 2015. A collection of papers presented at the 10th EUFOAM conference, Thessaloniki, Greece, 7–10 July 2014, edited by T. Karapantsios and M. Adler.
9. N. Kern, D. Weaire, A. Martin, S. Hutzler, and S. J. Cox. Two-dimensional viscous froth model for foam dynamics. *Phys. Rev. E*, 70:041411, 2004.
10. T. E. Green, A. Bramley, L. Lue, and P. Grassia. Viscous froth lens. *Phys. Rev. E*, 74:051403, 2006.